The *cryptocephal* Gene (ATF4) Encodes Multiple Basic-Leucine Zipper Proteins Controlling Molting and Metamorphosis in Drosophila

Randall S. Hewes, Anneliese M. Schaefer and Paul H. Taghert

Department of Anatomy and Neurobiology, Washington University School of Medicine, Saint Louis, Missouri 63110

Manuscript received January 13, 2000
Accepted for publication April 10, 2000

ABSTRACT

The *cryptocephal* (*crc*) mutation causes pleiotropic defects in ecdysone-regulated events during Drosophila molting and metamorphosis. Here we report that *crc* encodes a Drosophila homolog of vertebrate ATF4, a member of the CREB/ATF family of basic-leucine zipper (bZIP) transcription factors. We identified three putative protein isoforms. CRC-A and CRC-B contain the bZIP domain, and CRC-D is a C-terminally truncated form. We have generated seven new *crc* alleles. Consistent with the molecular diversity of *crc*, these alleles show that *crc* is a complex genetic locus with two overlapping lethal complementation groups. Alleles representing both groups were rescued by a cDNA encoding CRC-B. One lethal group (crc^{1}, crc^{R6}, and crc^{Rev8}) consists of strong hypomorphic or null alleles that are associated with mutations of both CRC-A and CRC-B. These mutants display defects associated with larval molting and pupariation. In addition, they fail to evert the head and fail to elongate the imaginal discs during pupation, and they display variable defects in the subsequent differentiation of the adult abdomen. The other group (crc^{R1}, crc^{R2}, crc^{E85}, crc^{E98}, and crc^{929}) is associated with disruptions of CRC-A and CRC-D; except for a failure to properly elongate the leg discs, these mutants initiate metamorphosis normally. Subsequently, they display a novel metamorphic phenotype, involving collapse of the head and abdomen toward the thorax. The *crc* gene is expressed throughout development and in many tissues. In third instar larvae, *crc* expression is high in targets of ecdysone signaling, such as the leg and wing imaginal discs, and in the ring gland, the source of ecdysone. Together, these findings implicate CREB/ATF proteins in essential functions during molting and metamorphosis. In addition, the similarities between the mutant phenotypes of *crc* and the ecdysone-responsive genes indicate that these genes are likely to be involved in common signaling pathways.

THE development of Drosophila and other insects is punctuated by several molts, during which the animal produces a new external cuticle and sheds the old one (Riddiford 1993). The larval molts are initiated and coordinated by steroid hormones, the ecdysteroids (hereafter called ecdysone). At the onset of metamorphosis, a high titer pulse of ecdysone triggers pupariation, which is followed ~12 hr later by a brief ecdysone pulse that causes head eversion and the prepupal-pupal transition. Subsequently, a large, prolonged surge of ecdysone directs adult development. These remarkable developmental changes involve the programmed cell death of most larval tissues, extensive remodeling of other larval tissues, and the generation of adult tissues from islands of undifferentiated imaginal cells (Riddiford 1993; Truman *et al.* 1994; Jiang *et al.* 1997).

Detailed studies of the responses to ecdysone in the larval salivary glands provided key insights into the gene regulatory pathways controlling molting and metamorphosis (Thummel 1996). Expression of a small set of about six early genes is triggered rapidly and directly by ecdysone. Together with ecdysone, these genes regulate numerous late genes. Four early genes have been molecularly characterized. *E74* encodes a family of ETS proteins (Burtis *et al.* 1990), *E75* encodes a family of orphan nuclear receptors (Segraves and Hogness 1990), the *Broad-Complex* (*BR-C*) encodes a family of zinc-finger proteins (DiBello *et al.* 1991), and *E63-1* encodes a novel Ca^{2+}-binding protein (Andres and Thummel 1995). *E74* and the *BR-C* control developmental responses to ecdysone in diverse larval and imaginal tissues (Kiss *et al.* 1988; Restifo and White 1991; Fletcher *et al.* 1995) at least in part through direct transcriptional regulation of the late genes (Urness and Thummel 1995; Crossgrove *et al.* 1996). Thus, the early genes are near the top of a complex gene regulatory hierarchy.

Mutations in several ecdysone-responsive genes reveal distinctive phenotypes that reflect important developmental functions. For example, an *E74B* mutant displays incomplete differentiation of the adult abdomen and failed gas bubble translocation at pupation (Fletcher *et al.* 1995). A mutation of β*FTZ-F1*, which functions as a competence factor for pupal stage-specific responses to ecdysone, displays similar translocation defects (Broadus *et al.* 1999). Mutations in *E74*, β*FTZ-F1*, and two other ecdysone-response genes, *crol* and *DHR3*, each display several additional common features. These

Corresponding author: Randall S. Hewes, Department of Anatomy and Neurobiology, Box 8108, Washington University School of Medicine, 660 S. Euclid Ave., St. Louis, MO 63110.
E-mail: hewesr@thalamus.wustl.edu

include defective eversion of the adult head and (with the exception of *DHR3*) incomplete leg disc elongation (Fletcher *et al.* 1995; D'Avino and Thummel 1998; Broadus *et al.* 1999; Lam *et al.* 1999). The head eversion defect is called the "cryptocephal" phenotype, named after *cryptocephal* (*crc*^{1}), a mutation that displays all of the above-mentioned defects (Hadorn and Gloor 1943). These phenotypic parallels indicate that *crc* and the ecdysone-response genes are likely to be involved in common regulatory pathways.

Fristrom (1965) examined chitin biosynthesis in the *crc*^{1} mutant and concluded that the head eversion defect is due to excess chitin deposition in (and increased stiffness of) the cuticle. Sparrow and Chadfield (1982) tested this hypothesis with a different *crc*^{1} strain and found normal chitin deposition. At pupation, *crc*^{1} mutants display contractions of the abdomen that are slower, more irregular, and weaker than in wild-type animals, indicating that behavioral abnormalities may cause at least some of the phenotypic defects observed in these mutants (Chadfield and Sparrow 1985). However, behavioral abnormalities likely do not explain other aspects of the *crc*^{1} mutant phenotype, such as incomplete abdominal differentiation. In a discussion of the similar phenotypic defects displayed by *E74B* mutants, Fletcher *et al.* (1995) hypothesized that premature muscle death accounts for the full range of defects observed in these cryptocephalic mutants. To distinguish among these and other competing models, it will be important to characterize *crc* gene function at the molecular and cellular level.

Here we show that *crc* encodes multiple proteins in the activating transcription factor 4 (ATF4) subfamily of CREB/ATF basic-leucine zipper (bZIP) transcription factors. ATF4 proteins have been implicated in several important developmental and disease processes, including wound healing (Estes *et al.* 1995), long-term synaptic facilitation (Bartsch *et al.* 1995), stress responses (Fawcett *et al.* 1999), apoptosis (Kawai *et al.* 1998), and cancer (Mielnicki *et al.* 1996). We add to this list by showing that the Drosophila ATF4 homologs play critical roles in molting and metamorphosis. We have isolated seven new *crc* alleles, which reveal multiple functions of the gene in larval molting, pupariation, pupation, and adult differentiation. These tissues include several targets of ecdysone signaling as well as the endocrine source of ecdysone, the ring gland. Our findings implicate CREB/ATF transcription factors for the first time in the hormonal regulation of molting and metamorphosis. Moreover, these results indicate that there are likely to be important interactions between signaling by *crc* and the ecdysone-response genes.

MATERIALS AND METHODS

Fly strains and culture: Flies were grown at 22°–24° on a standard cornmeal-yeast-agar medium. All crosses were performed at 25°. The *P{P-GawB}c929* insertion was generated in the laboratory of Dr. Kim Kaiser (University of Glasgow). The *w; Sp/CyO; P[629-1N]* stock contains an insertion of the GAL4 coding region fused to the *hsp70* promoter (Halfon *et al.* 1997). All other mutations are described in Lindsley and Zimm (1992) or FlyBase (Gelbart *et al.* 1997) and were obtained from the Bloomington Drosophila stock center and other sources.

Molecular biology: Standard molecular biology techniques were performed as described in Sambrook *et al.* (1989). Single-fly PCR (Gloor *et al.* 1993) was conducted on larvae, adult males, or virgin females. Plasmid rescue of *c929* (Pirrotta 1986) was used to generate probes for screening phage λEMBL3 and cosmid CoSpeR genomic libraries. The phylogenetic analysis was performed using FITCH software (Dayhoff PAM matrix; Felsenstein 1993). For cDNA isolation, probes were prepared from the plasmid rescue fragment and two *Sac*I fragments (3.2 and 5.7 kb) flanking the *c929* insertion site. These probes were used to screen cDNA libraries made from adult heads (>750,000 plaques) and 0–24-hr embryos (>250,000 plaques).

Sequencing of the *crc*^{1} allele was performed on the products of at least two independent PCR reactions from single *y w; crc*^{1}*/crc*^{1} larvae. The genomic region containing exons 5 and 6 was amplified using the oligonucleotides 5′-AGCGCTC GAATTGTATCTCGGCTTT-3′ and 5′-AAGCTGGCAGACTT GATTAGCTAACT-3′. The genomic region containing exons 7 and 8 was amplified using 5′-GACCAAAAGGCAACG TTGAACTGCAT-3′ and 5′-GGACAGGCTGCGTACTTTGG TGATT-3′. Except for short regions near the template ends, the sequencing was performed on both strands. In addition to the Q^{171}R mutation described in results, we identified the following six polymorphisms and two conservative substitutions (the second base of each pair listed in parentheses refers to the sequence of the *crc*^{1} chromosome): confirmed polymorphisms, TCGAATTG(T/A)ATCTCGGC (5′untranslated region [UTR]), GTGTATCA(A/T)TTAAAATA (5′ UTR), TTTACCGT(T/C)TTAATTTT (5′ UTR), GGAGCGGC(G/A) CAACGAAA (open reading frame; H^{354}R), CAGCTGAT(C/T) CGAGAGTT (open reading frame; I^{364}I), GGCTTTAT(G/T) TTCTTTGA (3′ UTR); potential mutations, ATCTTCAT(T/A) ATATAAGG (5′ UTR), TTTCAGCC(T/G)AACATTAA (open reading frame; P^{107}P).

Microscopy and photography: Preparations were imaged on a Zeiss Axioplan fitted with a SPOT CCD camera and software (Diagnostic Instruments, Sterling Heights, MI). Live pupae were imaged with a Sony CCD-IRIS video camera.

Germ-line transformation: Germ-line transformation was performed as described (Benveniste and Taghert 1999) using a pP{UAS-*crc*} expression plasmid containing a 2.5-kb insert ligated into the *Eco*RI to *Not*I sites of the pP{UAST} expression vector (Brand and Perrimon 1993). The insert was made through fusion of two cDNAs at an internal *Eco*RI site in exon 5a. We obtained two independent insertions, and additional independent insertions were created by transposition of these onto a chromosome bearing the *crc*^{Rev8} mutation.

Generation of *crc* deletions: We generated white-eyed revertants of *c929* as described (O'Brien *et al.* 1994) and molecularly screened 37 for deletions of *crc*. One deletion, *Rev8*, was identified. *Rev8* was mapped by Southern blot and by PCR on *y w; Rev8/Df(2L)Rev4* larvae. We also generated deletions by imprecise excision and *P*-induced male recombination (Preston *et al.* 1996) using an *al dp c929 px sp* chromosome. We screened 104 hemizygous revertant F_2 males by single-fly PCR, and we characterized 15 independent recombinants (Sved *et al.* 1990) by Southern blot analysis and PCR. Five deletions of *crc* were identified in this screen (*R1*, *R2*, *R6*, *E85*, and *E98*).

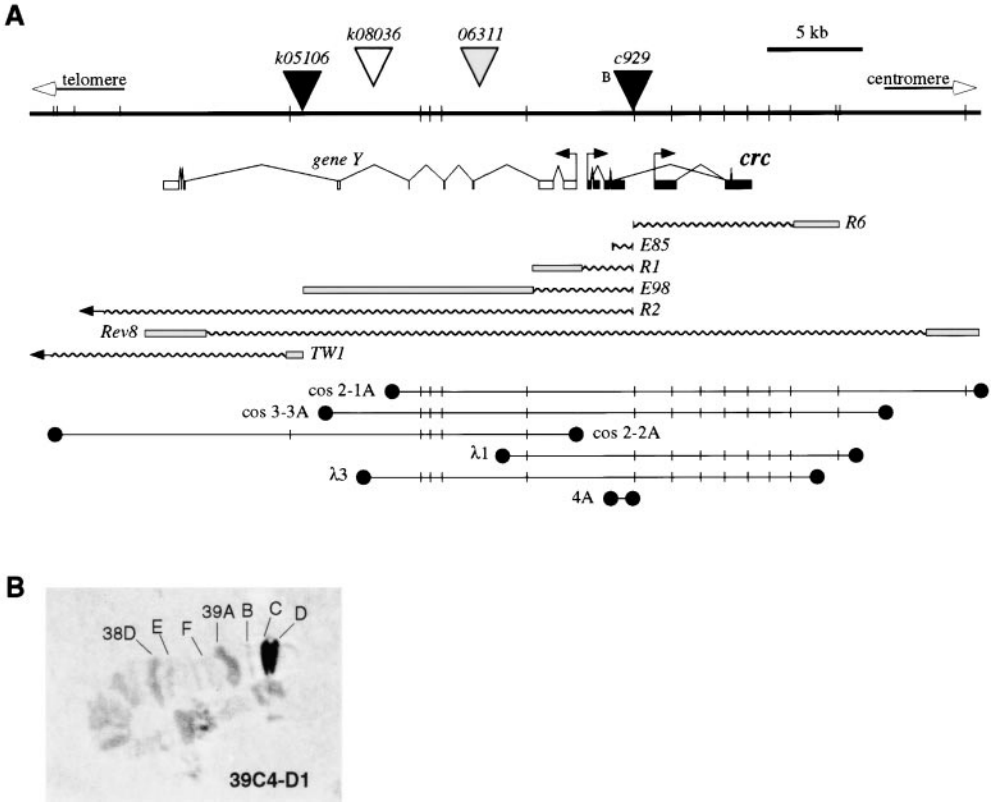

Figure 1.—Genomic organization of 39C4. (A) The organization of *crc* and *gene Y* is shown in simplified schematic organization with the direction of transcription indicated (arrows). Deletions are indicated as wavy lines; the shaded bars and arrows indicate breakpoint uncertainties. Other deficiencies of the entire region were used (*e.g.*, *Rev4* and *TW161*) but are not shown. *P* elements are indicated with triangles. Phage (λ), cosmid (cos), and plasmid rescue (4A) clones used to construct the walk are shown below. *Eco*RI sites determined by restriction mapping are shown as tick marks on the genomic clones and as half-tick marks below the top line. The half-tick marks above the top line represent *Eco*RI sites predicted from the DS01560 sequence. On the proximal side of *crc*, there were no ESTs or clear gene homologies (other than transposons) within 20 kb. B, pBluescript side of *c929*; black triangles, known insertion sites (Spradling *et al.* 1999); gray triangle, tentative location mapped by Southern blot and *in situ* hybridization (Spradling *et al.* 1995); white triangle, location inferred from complementation analysis. (B) *In situ* hybridization to polytene salivary chromosomes using cos 2-1A as a probe. Other genomic clones from the chromosomal walk also hybridized to overlapping segments of 39C-D (not shown).

R1, *R2*, and *c929* were backcrossed to $y\ w^{67c23}$ for 7 generations, and *R6* was backcrossed to $y\ w^{67c23}$ for 14 generations. Unless noted otherwise, these recombined chromosomes were used for all subsequent experiments.

mRNA *in situ* hybridization: Whole-mount *in situ* hybridization was performed on stage 1–16 embryos and on larval tissues (Tautz and Pfeifle 1989). We prepared the probes from a cDNA subclone containing sequence between the *Cla*I site in exon 7 and the *Eco*RI site in exon 8. This sequence is common to the *crc*-a, *crc*-b, and *crc*-c mRNAs and encodes amino acids 98–373; it includes the bZIP domain and the first 218 bp of the 3′ UTR, but no sequence corresponding to *crc*-d.

RESULTS

Molecular cloning of *crc*: The cytological location of crc^1 is 39C2-4 (Wright *et al.* 1976). We initiated the cloning of crc^1 using a *P*-element insertion, *c929*, which we mapped to 39C4 by *in situ* hybridization. Subsequent to plasmid rescue, we obtained several overlapping genomic clones covering a region of ~50 kb (Figure 1A). The DS01560 Berkeley Drosophila Genome Project (BDGP) clone covers this region (GenBank accession no. AC005130).

We isolated seven cDNAs from diverse libraries (see materials and methods). All were products of the same gene, which we named *crc* (GenBank accession nos. AF201914–AF201924). These clones represent six distinct mRNAs (Figure 2A). Southern analysis showed that the *crc* locus is represented only once in the genome (data not shown). The BDGP has generated >40 *crc* expressed sequence tags (ESTs) derived from several stages and tissues, indicating *crc* expression throughout development. Among clones from adult head and embryo cDNA libraries, the isoforms *crc*-a and *crc*-b are the most abundant, representing ~85% and ~10% of the total, respectively. Each of the other *crc* mRNA isoforms is represented by a single cDNA.

The predicted *crc* open reading frames are shown in Figure 2B. CRC-A is encoded by *crc*-a, whereas *crc*-b and *crc*-c encode an identical isoform, CRC-B. CRC-A and CRC-B differ only at the N terminus. The *crc*-d transcript encodes CRC-D, a truncated isoform of CRC-A. The C terminus of the 288-amino acid region common to CRC-A and CRC-B contains basic DNA-binding and leucine zipper protein dimerization motifs (Figure 2B). The basic DNA-binding region is immediately preceded by a PEST-like sequence (PEST score 8.21, Rodgers *et al.* 1986). Thus, CRC may display PEST-mediated instability.

The bZIP domain of CRC displays the strongest homology with other members of the CREB/ATF superfamily of transcription factors. CRC belongs to the ATF4 subfamily, on the basis of phylogenetic analysis (Figure

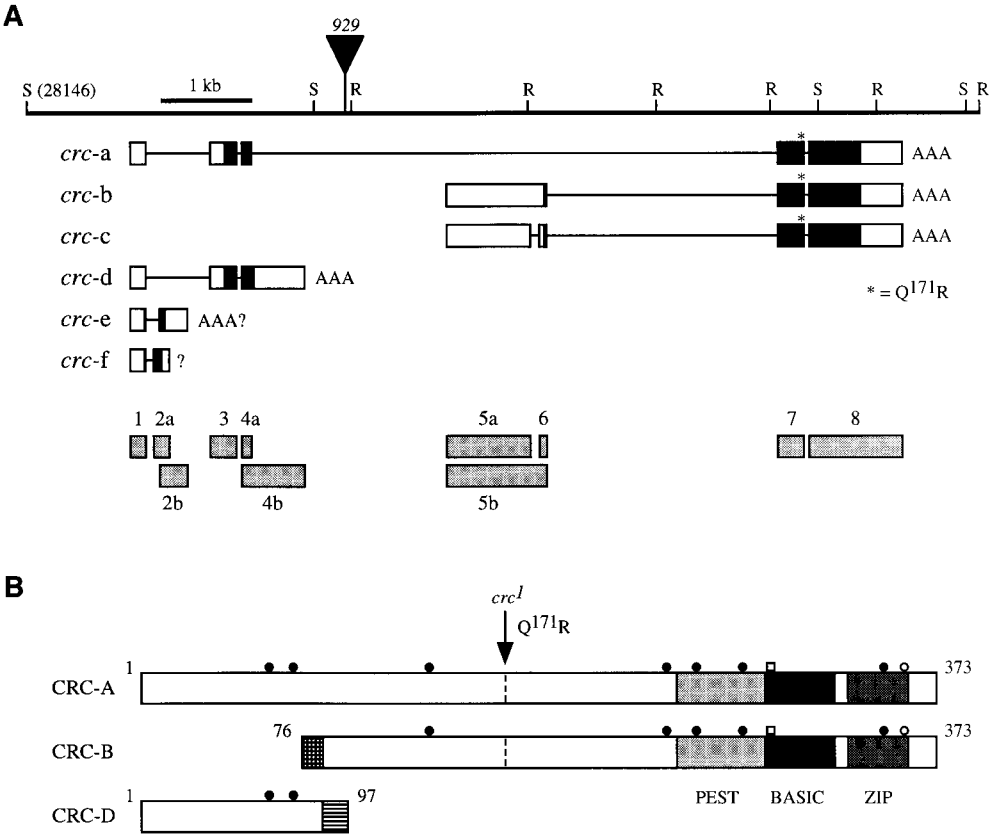

Figure 2.—*crc* encodes at least six mRNA and three protein isoforms. (A) Exons and introns of the *crc* transcripts are shown as boxes and horizontal lines, respectively. The putative open reading frames (black) and untranslated regions (white) are indicated. Exons were numbered as indicated below (gray boxes). The predicted translational starts of *crc*-a/d and *crc*-b contain Cavener consensus sequences (Cavener and Ray 1991) and are preceded by stop codons in each reading frame. (B) Organization of the three predicted protein isoforms. Hatched boxes, isoform-specific sequences; S, *Sac*I; R, *Eco*RI; closed circles, consensus casein kinase II phosphorylation sites; open circles, consensus tyrosine kinase phosphorylation site; open squares, consensus cAMP/cGMP-dependent kinase phosphorylation site; PEST, putative protein degradation signal; BASIC, basic DNA-binding region; ZIP, leucine zipper.

3A) and the conservation of several characteristic residues in the bZIP domain (Figure 3B). CRC is most closely related to mouse and human ATF-4 (>40% sequence identity within the bZIP domain); CRC is much more distantly related to Drosophila CREB-A and CREB-B (Figure 3A).

Generation of *crc* alleles: We generated additional *crc* alleles using imprecise *P*-element excision and male recombination. We found six partial or complete deletions of *crc* (Figure 1A). crc^{Rev8} (*Rev8*) is a complete null; it removed all of the *crc* exons and several exons from *gene Y*. The remaining five deletions (*R1, R2, R6, E85,* and *E98*) are all partial disruptions of *crc*. At least two of these alleles, *R2* and *E98*, also disrupt *gene Y*. *E85* appears to be a specific CRC-D mutant, since it affects only exon 4b. By contrast, *R1, R2,* and *E98* disrupt both CRC-A and CRC-D. *R6*, which deleted the exons encoding the bZIP domain, disrupts CRC-A and CRC-B. Because exons 1–4 remain intact in *R6*, this allele may not disrupt CRC-D and two small 5′ RNAs (*crc*-a and *crc*-f).

R1, R2, R6, and *E98* each retained some or all of *c929*, the *P* element used for the mutant screens. In *E85*, *c929* appears to have been excised completely. An additional recombinant line, *R20*, contained a precise excision of *c929*.

Complementation analysis of the *crc* alleles: Complementation analysis revealed at least three lethal groups in 39C2-4, two of which (the "5′ group" and "3′ group") were associated with deletions of *crc* exons (Tables 1 and 2). The 5′ group includes *R1, R2, E85,* and *E98*, all deletions of 5′ *crc* exons, as well as crc^{929} (*929*). The 3′ group includes crc^{1} and *R6*, a deletion of the 3′ *crc* exons. A third lethal complementation group was associated with disruptions of *gene Y* (Table 3).

With the exception of crc^{1}, all of the *crc* mutant alleles share the same parental chromosome, *929*. Precise excision of the *c929 P* element (*R20*) fully restored the viability of animals bearing this chromosome *in trans* over *Rev8*, a lethal deletion of the entire *crc* locus (Figure 1A), and over *Rev4*, a larger deletion of 39C (Table 1). Thus, the parental *929* chromosome displayed no lethality in 39C2-4 independent of the *P*-element insertion.

The *crc* 5′ complementation group was associated with isoform-specific disruptions of the *crc* gene. For example, *929* was semilethal *in trans* over *TW161, Rev4,* and *Rev8* (all of which completely delete *crc*) but not over *TW1*, which leaves intact the entire *crc* gene as well as ~15 kb of DNA upstream of the putative *crc*-a transcriptional start site (Table 1). Since the *929 P* element is inserted in an intron of *crc* upstream of the putative *crc*-b/c transcriptional start site (Figure 2A), the lethality caused by *929* may reflect a specific disruption of the *crc*-a mRNA isoform. We obtained similar results with *R1*, which deletes all of the 5′ exons of *crc* (leaving the exons encoding *crc*-b and *crc*-c intact). Both *R1* and *929* displayed similar lethality (with variable penetrance) in crosses to the deficiencies *TW161, Rev4,* and *Rev8*. *R1* was semilethal in homozygotes, whereas *929* homozygotes were fully viable. Thus, *R1* appears to

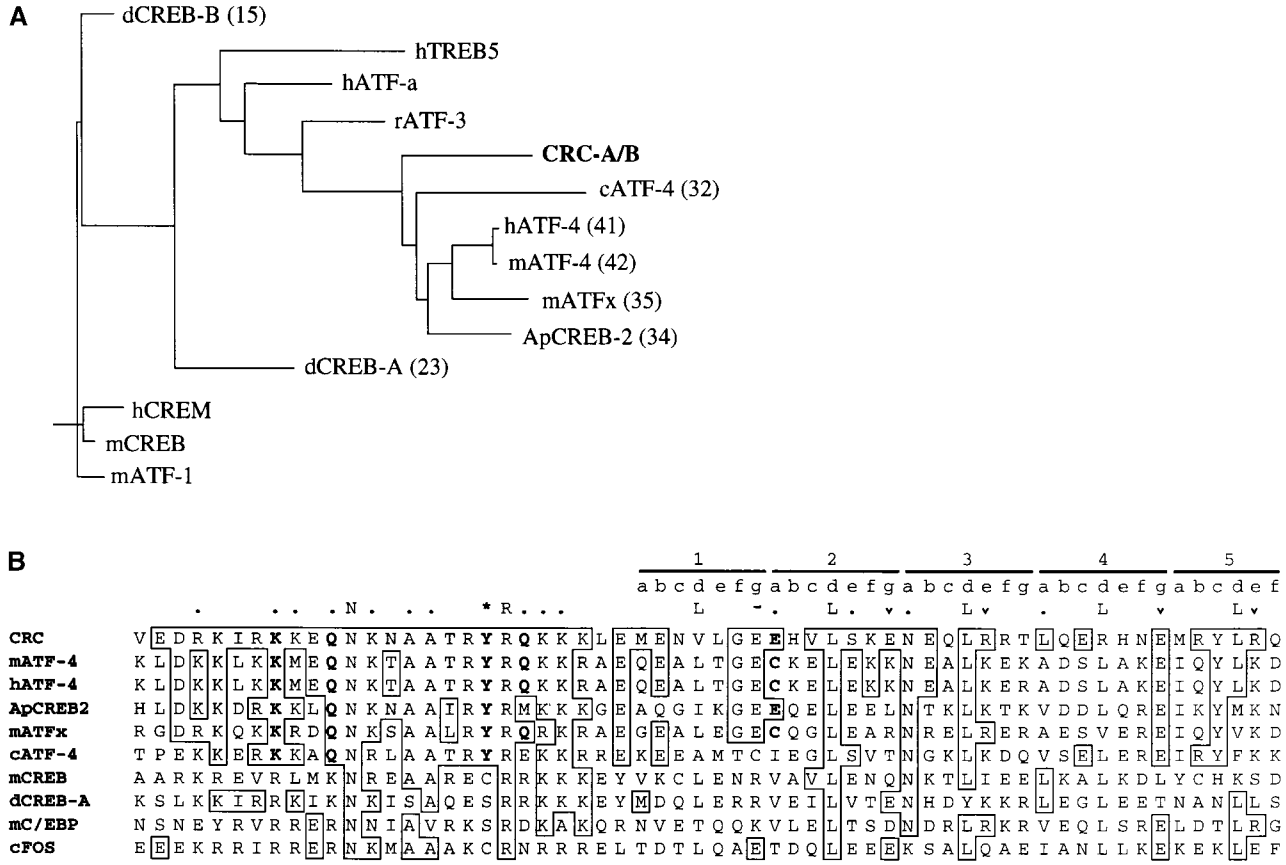

Figure 3.—CRC is the Drosophila homolog of ATF4, a member of the CREB/ATF family of transcription factors. (A) An unrooted phylogenetic tree for CREB/ATF bZIP domains. Proteins separated by shorter horizontal branches are more closely related. Percentage identities between CRC-A/B and other bZIP domains are shown in parentheses. (B) Alignment of selected bZIP domains. Positions marked by boldfaced letters distinguish members of the ATF4 subfamily from other bZIP proteins. The numbers and lowercase letters to the upper right indicate the heptad repeats of the leucine zipper (see Vinson *et al.* 1993). Dots, residues strongly conserved in bZIP proteins; N and R, strictly conserved residues; asterisk, strictly conserved C or S residue (except in the ATF4 subfamily); L, positions of zipper leucines; -, acidic residue available for interhelical salt bridge in heterodimers; inverted carets, residues available for interhelical salt bridges in CRC homodimers. Sequence accession nos.: dCREB-B, Drosophila CREB-B (AH004367); hTREB5, human TREB5 (NM 005171); hATF-a, human ATFa (NM 006856); rATF-3, rat ATF3 (P29596); cATF-4, *Caenorhabditis elegans* ATF-4 (CAA93757); hATF-4, human ATF-4 (P18848); mATF-4, mouse ATF-4 (CAA43723); mATFx, mouse ATFx (AAB21705); ApCREB-2, Aplysia CREB-2 (U40851); dCREB-A, Drosophila CREB-A (M87038); hCREM, human CREM (NM 001881); mCREB, mouse CREB (Q01147); mATF-1, mouse ATF-1 (P81269); mC/EBP, mouse C/EBP (M62362); cFOS, chicken cFOS (M37000).

be a slightly more severe allele. This difference may stem from the fact that *R1* disrupts the *crc*-d-f mRNAs in addition to *crc*-a (Figure 2A). Consistent with this hypothesis, *E85*, a smaller deletion that disrupts an exon specific to *crc*-d, displayed significant lethality *in trans* with *TW161* and *Rev4* (Table 1). The *E85* chromosome also appears to bear a lethal mutation at a second, distant site: *E85* homozygotes displayed greater lethality than *E85* hemizygotes, and in contrast with the larger *R1* deletion, *E85* displayed some lethality *in trans* with *TW1*. Finally, there were two stronger lethal alleles, *E98* and *R2*, and the degree of lethality associated with these alleles (Table 1) was correlated with the distal extent of these deletions (Figure 1A).

The *crc* 3′ complementation group was associated with disruptions of both of the major *crc* mRNA isoforms, *crc*-a and *crc*-b. *R6* deletes all of the 3′ *crc* exons shared by these two mRNAs. crc^1 and *R6* both were lethal *in trans* with deletions of the *crc* locus (Table 1), and crc^1 and *R6* failed to complement each other. By contrast, crc^1 was fully viable over deletions that extend distally from the *c929 P*-element insertion site (Tables 1 and 2). Thus, the wild-type function(s) of the *crc* gene must include contributions by transcription units located proximal to the *c929* insertion, such as *crc*-b and *crc*-c. We observed up to 2% adult escapers among hemizygous crc^1 progeny (Table 2; see Figure 5A). Hemizygous *R6* adult escapers were never observed. Thus, although both crc^1 and *R6* are very strong hypomorphs, we conclude that *R6* is a more severe allele. *R6* is not a complete *crc* amorph, since it complements *E85*.

The 5106/8036 complementation group maps to a separate gene: BDGP ESTs identify a novel gene (*gene Y*) located ~820 bp distal to *crc*, and we identified three

TABLE 1

Complementation of *crc* alleles with deficiencies of 39C4

Lethal group	Female	Male: Deficiencies of 39C4 *TW1*	*TW161*	*Rev4*	*Rev8*	Male: Self
Wild-type	*R20*			92	85	
crc null	*Rev8*	0***	0***	0***	0***	
crc 5′	*929*	100	7***	13***	37***	104
	R1	123	53***	21***	17***	45***
	E85	75*	57***	57***		37***
	E98	14***	0***	6***	0***	0***
	R2	0***	0***	0***	0***	0***
crc 3′	crc^1	120	0***	0***	0***	0***
	R6	93	0***	0***	0***	0***

The female genotype in each cross is indicated in the second column, and the male genotype is listed above columns 3–7. The results of each cross are listed as a percentage of the expected Cy^+ progeny (calculated from the number of Cy^- progeny). Most stocks were *y w* and were balanced with *SM6* or *CyO*, y^+ (*R20* and *E85*, only). *TW1* and *TW161* (breakpoints: 38A6 and 40A4-B1; see Lindsley and Zimm 1992) were balanced over *CyO*. *Rev4* is a deletion of 39C1-39C4 (39B1-B2 is probably intact, A. Carpenter, personal communication; data not shown). The total number of progeny scored for each cross was 104–327; for the large majority, the total was >200. Self, male, and females were the same genotype; asterisks, significant deviation from the null hypothesis (*** $P < 0.001$, or * $P < 0.05$).

independent *P*-element insertions in or near this gene (Figure 1A). The *06311* insertion was fully viable *in trans* with deletions of 39C (Table 3). The other two insertions, *l(2)k05106* and *l(2)k08036*, form a lethal complementation group ("5106/8036"; Spradling *et al.* 1995) that was independent of the 5′ and 3′ groups of *crc* alleles (Table 3). *TW1*, with a breakpoint ~15 kb distal to *crc* (Figure 1A), uncovers the 5106/8036 group (Table 3) but does not uncover crc^1 (Table 1). The 5106/8036 group includes *R2* and *E98*, but it does not include *R1*. Finally, *l(2)k05106*, *l(2)k08036*, *R2*, and *E98* all fully complement crc^1, and *l(2)k05106* and *l(2)k08036* complement *R6*, a deletion of the *crc* bZIP domain. Therefore, *l(2)k05106* and *l(2)k08036* are not *crc* alleles, and the 5106/8036 group corresponds either to disruptions of *gene Y*, or another, more distally located gene.

TABLE 2

Complementation among *crc* alleles

Lethal group	Female	Male: crc^1	Male: *R6*
crc null	*Rev8*	1***	0***
crc 5′	*929*	93	21***
	R1	119	19***
	E85	92	108
	E98	117	19***
	R2	89	4***
crc 3′	crc^1	0***	1***
	R6	0***	0***

The female genotype in each cross is indicated in the second column, and the male genotype is listed above columns 3 and 4. The results are summarized as in Table 1. The total number of progeny scored for each cross was 157–295; for the large majority, the total was >200. Asterisks, significant deviation from the null hypothesis (*** $P < 0.001$).

Phenotypic analysis of the 3′ group of *crc* alleles: The crosses shown in Tables 1 and 2 revealed two largely distinct phenotypes, each generally associated with only one of the *crc* complementation groups. This result further indicates that the 5′ and 3′ groups represent distinct genetic functions. For the 3′ group (crc^1 and *R6*), there were several lethal phases during larval, pupal, and adult development. Both crc^1 and *R6* hemizygotes displayed 15–50% of their lethality after pupariation. At each stage, the *R6* allele displayed a more severe phenotype than crc^1.

The molts between successive larval stages were disrupted in crc^1 mutants, and this phenotype was accompanied by significant lethality (Chadfield and Sparrow 1985). We observed a comparable phenotype in the *R6* mutants (Figure 4G), and the presence of supernumerary mouthparts was strongly correlated with larval lethality (data not shown). In addition to the larval molting defects, *R6* hemizygotes showed delayed and defective pupariation. By contrast, crc^1 hemizygotes pupariated normally (*cf.*, Hadorn and Gloor 1943), consistent with the weaker hypomorphic phenotype of crc^1 (Table 2). Although ~5% of the hemizygous *R6* puparia were indistinguishable from wild type, the rest were aberrant to varying degrees. These defects included a failure to evert the anterior spiracles and a retention of a larval shape, which was thinned, elongated, and sometimes curved to one side (Figure 4H). In the most severe cases,

TABLE 3

Complementation analysis of *gene Y* alleles

Lethal group	Female	Male									
		TW1	*TW161*	*Rev4*	*Rev8*	*Self*	*crc*^{1}	*R6*	*R1*	*R2*	*E98*
5106/8036	*06311*	85	104	86	121	0***	104	84			
	k05106	0***	1***	28***	15***	2***	108	114	96	21***	46***
	k08036	9***	5***	43***	42***	15***	115	88	82	17***	48***

The female genotype in each cross is indicated in the second column, and the male genotype is listed above columns 3–12. The results of each cross are listed as a percentage of the expected Cy^{+} progeny (calculated from the number of Cy^{-} progeny). The *06311* stock was *y w* and was balanced with *SM6*. The *k05106* and *k08036* stocks were *w* and were balanced with *SM6*. The total number of progeny scored for each cross was 115–346; for the large majority, the total was >200. Self, male and females were the same genotype; asterisks, significant deviation from the null hypothesis (*** $P < 0.001$).

the abdominal gas bubble, which normally forms ~6 hr after pupariation (Bainbridge and Bownes 1981), did not appear, although the larval mouthparts were later expelled.

crc^{1} and *R6* mutant pupae displayed a range of defects associated with pupation and subsequent development (Figure 4, A–D; Table 4), as previously described for the *crc*^{1} allele (Hadorn and Gloor 1943; Fristrom 1965; Chadfield and Sparrow 1985). The pupal phenotypes of these two alleles were similar. The mutants often failed to expel or translocate the abdominal gas bubble. Head eversion failed or was incomplete, and the leg and wing discs did not completely elongate. In addition, segmentation and differentiation of the abdomen usually failed, although in some cases the anterior abdominal segments differentiated (Figure 4B). Other aspects of adult development proceeded normally, resulting in the appearance of mature eye pigments and darkened macrochaetes and differentiation of the wings and legs (Figure 4, A–D).

Adult, hemizygous *crc*^{1} females displayed markedly decreased fecundity. In addition, 5–50% (depending upon the genetic background) of the hemizygous *crc*^{1} adults of both sexes failed to expand their wings and

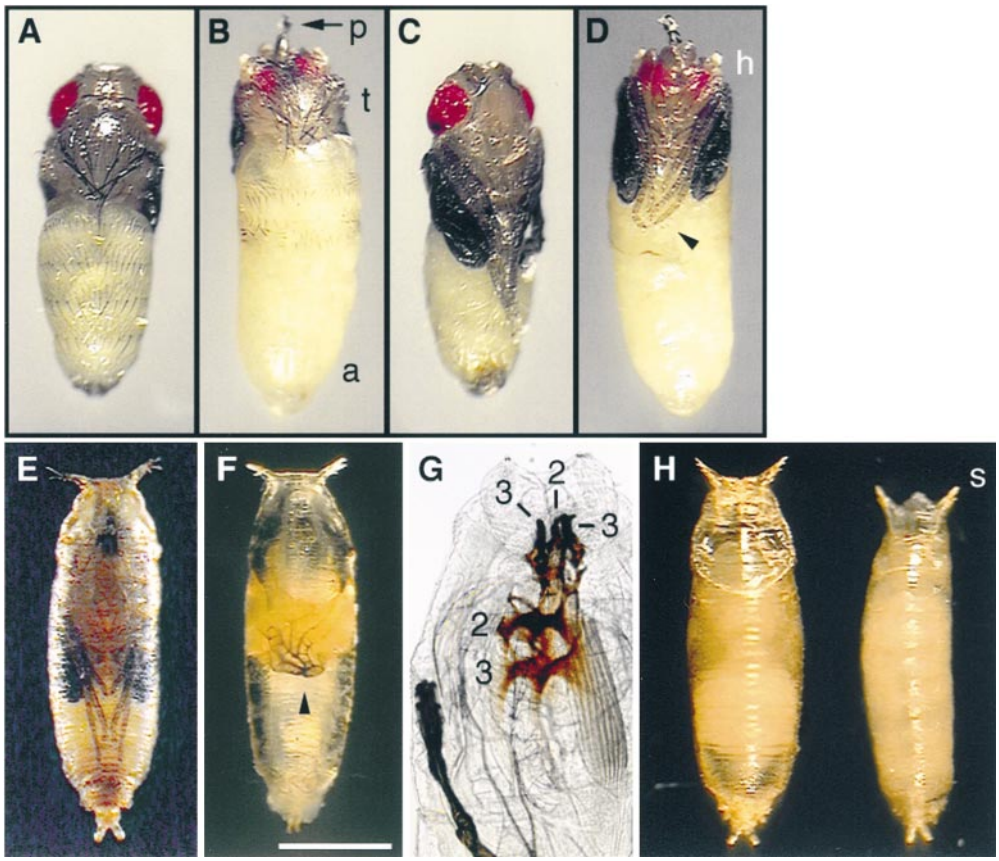

Figure 4.—Morphological defects associated with mutations in the 39C4 region and *crc*-c misexpression. In A–D, the puparium was removed (the pupal cuticle was left intact). In E–H, animals were photographed through the puparium. (A) Wild-type, dorsal view. (B) *crc*^{1}/*Rev4*, dorsal view. (C) Wild type, ventral view. (D) *crc*^{1}/*Rev4*, ventral view. (E) Ventral view of a wild-type pharate adult. (F) Ventral view of a *R2/R6* pupa displaying the head/abdomen-collapsed phenotype. (G) Multiple mouthparts in a third instar *y w; R6/Rev8* larva. (H) Dorsal views of a *Rev8 or R6/CyO, y*$^{+}$ pupa (left) and a *R6/Rev8* sibling (right). p, larval mouthparts; t, reduced thorax; a, naked, unsegmented abdomen; h, cryptocephal head; 3, third instar mouthparts; 2, second instar mouthparts; s, partially everted anterior spiracle; arrowheads, incompletely elongated legs. Bar, 1 mm (in G, 0.19 mm).

TABLE 4

Pupal phenotypes associated with *crc* alleles

		Male			
		Deficiencies of 39C4		*crc* 3′ alleles	
Lethal group	Female	*Rev4*	*Rev8*	*crc*^{1}	*R6*
crc null	*Rev8*	early	early	crc	crc
crc 5′	*929*	hac	hac		hac
	R1	hac	hac		hac
	E85	hac	ND		
	E98	hac	hac		hac
	R2	early	hac		hac
crc 3′	*crc*^{1}	crc	crc	crc	crc
	R6	early	crc	crc	early

The pupal phenotypes for a subset of the crosses shown in Tables 1 and 2 are indicated with the following codes: crc, cryptocephal; hac, head/abdomen-collapsed; early, lethality prior to the pupal stage. The pupal phenotypes of viable allelic combinations were not scored. ND, not done.

fully tan the adult cuticle. Other hemizygous *crc*^{1} adults displayed more subtle defects involving the wings, legs, scutellum, scutellar bristles, halteres, and dorsal thorax. Many of these defects could be explained by incomplete tanning of the adult cuticle after eclosion.

Phenotypic analysis of the 5′ group of *crc* alleles: The lethal phase for the 5′ group of *crc* alleles (*R1*, *R2*, *E85*, *E98*, and *929*) was primarily after pupariation, since the number of dead pupae observed on the sides of the vials was approximately equal to the total amount of lethality. We did not observe larvae with multiple mouthparts, and the puparia were normal in size and shape (Figure 4F). In addition, gas bubble translocation, expulsion of the larval tracheae and mouthparts, and head eversion were all completed successfully. The 5′ group of alleles displayed defects in leg and wing disc elongation that were similar to those observed for the 3′ group, but they also caused novel defects in adult development ("head/abdomen-collapsed" phenotype; Table 4). In contrast to *crc*^{1} (Figure 4, A–D), the distal portions of the everted leg discs often darkened abnormally and did not differentiate further. After pupation, the abdomen shrank markedly and withdrew to a dorsal position. Subsequently, the head collapsed partially or completely into the thoracic cavity (Figure 4F). Despite these events, many pupae developed eye pigmentation and other signs of adult differentiation.

Phenotypic overlap between the 5′ and 3′ *crc* complementation groups: Although most of the mutations within the 5′ group fully complemented the 3′ group, *R6* was an exception. *R6* uncovered *crc*^{1} (3′ group) as well as *R1*, *R2*, *E98*, and *929* (5′ group; Table 2). In addition, *R6* mutants displayed a cryptocephal phenotype when crossed to *crc*^{1} and the head/abdomen-collapsed phenotype when crossed to alleles from the 5′ group (Table 4). When placed *in trans* with *R6*, the *929*, *R1*, *R2*, and *E98* alleles each displayed a similar degree of lethality (independent of deletion size), indicating that each of these crc 5′ alleles displayed comparable defects in the function of the *crc* gene.

Interestingly, the 5′ group alleles and *R6* (but not *crc*^{1}) also displayed the head/abdomen-collapsed phenotype when heterozygous over either *CyO, y*$^+$ or a second balancer, *In(2LR)SLM*. This dominant effect was associated with variable, but significant pupal lethality. Because the *CyO, y*$^+$ and *In(2LR)SLM* chromosomes were created independently (I. Duncan, personal communication), it appears unlikely that these chromosomes share dominant enhancers of the head/abdomen-collapsed phenotype. Rather, this result suggests that the 5′ group alleles and *R6* are *crc* haploinsufficient in some genetic backgrounds.

Sequencing of the *crc*^{1} allele: Because deletions distal to *c929* complemented *crc*^{1} (Table 2), we sequenced the genomic regions containing exons 5 and 6 and exons 7 and 8 from *crc*^{1}/*crc*^{1} larvae. We identified nine differences between the *crc*^{1} and wild-type sequences. Of these, six corresponded to wild-type polymorphisms, and two were conservative substitutions (see materials and methods). The remaining substitution (GATGCA CAGCCAAAA; the underlined residue is G in *crc*^{1}) results in a nonconservative change from glutamine to arginine ($Q^{171}R$; Figure 2). Because $Q^{171}R$ was the only nonconservative substitution in the *crc*^{1} coding sequence, we speculate that it is the cause of the associated phenotypic defects.

Rescue of *crc* lethality by germ-line transformation: To confirm the molecular identification of the *crc* gene, we rescued the lethality of mutant *crc* alleles using germline transformants expressing a *crc* cDNA. On the basis of the complementation analysis, we predicted that ectopic expression of the CRC-B protein isoform (encoded by the *crc*-c mRNA, Figure 2) would rescue *crc*^{1} lethality. To test this hypothesis, we made multiple independent germ-line transformants with *crc*-c under the control of a GAL4 upstream activating sequence (*UAS-crc*). In six of seven lines, *UAS-crc* rescued 8–21% of the lethality in *crc*^{1}/*Rev8* heterozygotes (Figure 5A). The rescue was constitutive (without heat shock), presumably reflecting basal expression of *UAS-crc*. Heat-shock-induced expression of *UAS-crc* under the control of an hs-GAL4 driver caused substantial lethality in an otherwise wild-type background; thus the hs-GAL4 driver only lowered the degree of rescue seen (data not shown). The degree of rescue also was influenced by the parental genotype; for insertion *9-2*, ~40% rescue was obtained when both parental stocks were balanced with *CyO, y*$^+$ (data not shown).

We also attempted rescue of 5′ group functions. We chose *929* as a representative 5′ group allele for two reasons. First, the complementation (Tables 1 and 2) and molecular (Figure 2) analyses indicated that *929*

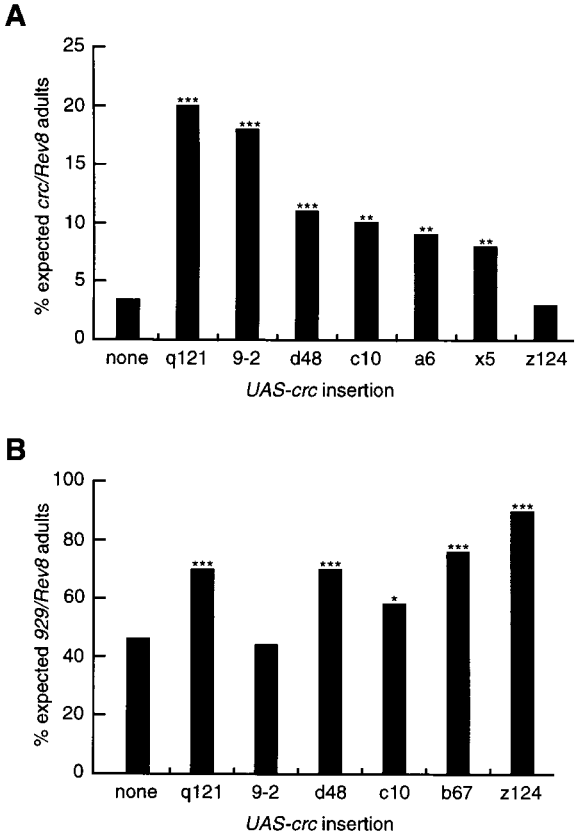

Figure 5.—Rescue of crc^1 and *929* lethality by multiple independent *UAS-crc* lines. (A) Rescue of $crc^1/Rev8$ by *UAS-crc*. The parental female genotype was *y w;* $crc^1/SM6$. (B) Rescue of *929/Rev8* by *UAS-crc*. The female parents were *y w;* crc^{929}. In A and B, the expected number of Cy^+ adults in each cross was calculated from the number of Cy^- siblings. χ^2-tests were performed assuming that 3% (A) or 46% (B) of the hemizygous mutants would survive to the adult stage without rescue. All crosses were maintained at 25°. The parental male genotypes were *y w; Rev8, UAS-*crc^x*/CyO,* y^+, where *x* indicates one of nine independent *UAS-crc* lines (none = no insertion). For line *9-2,* the parental males were *y w; Rev8/CyO,* y^+; *UAS-*$crc^{9\text{-}2}/+$. The total progeny in each cross was as follows (listed in order: A, B): none (695, 198), q121 (381, 180), 9-2 (203, 382), d48 (423, 339), c10 (103, 328), a6 (110, 112), x5 (73, 149), b67 (332), z124 (380, 338). * $P < 0.05$; ** $P < 0.01$; *** $P < 0.001$.

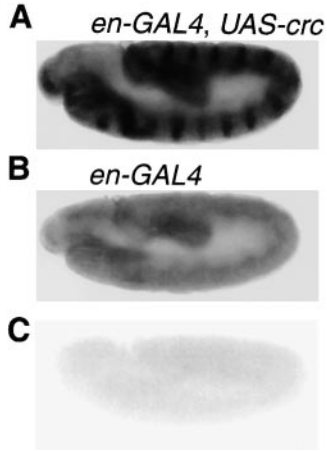

Figure 6.—Whole-mount *crc in situ* hybridization in stage 12 embryos. All of the embryos carried a single copy of the *en-GAL4* insertion, and approximately half of the embryos carried a copy of the *UAS-*$crc^{9\text{-}2}$ insertion (the other half carried a wild-type third chromosome). (A and B) Antisense *crc* RNA probe. (C) Sense probe.

displayed lethality due to disruption of *crc*-a without any confounding disruption of *gene Y*. Second, *c929* is a GAL4 enhancer trap *P* element, which allowed heterogeneous expression of the *UAS-crc* transgene in *929* mutants. The *c929* GAL4 reporter gene is expressed in larvae in peptidergic central nervous system (CNS) neurons, intrinsic cells of the ring gland, salivary gland, fat body, patches of the epidermis, the PM peritracheal cells, and a few other scattered locations (Schaefer and Taghert, *Society for Neuroscience Abstract* 1995; O'Brien and Taghert 1998; R. S. Hewes and P. H. Taghert, unpublished results). By contrast, there is very restricted *c929* reporter gene expression in the imaginal discs and no detectable expression in the skeletal muscles and abdominal histoblasts. Several independent *UAS-crc* insertions partially or completely rescued the lethality observed in *929* hemizygotes (Figure 5B). Thus, there were two separable *crc* functions, and both were rescued by transgenic expression of CRC-B. Moreover, given the inclusion of numerous neurosecretory neurons in the pattern of *c929* reporter gene expression, we speculate that *crc* may function in close association with ecdysone biosynthesis/secretion. This issue will be examined in detail in future studies.

Expression pattern of *crc* transcripts: We performed *in situ* hybridization to determine the expression pattern of *crc* mRNAs. We first tested the specificity of the probes on embryos expressing *UAS-crc* under the control of an *engrailed-GAL4* (*en-GAL4*) driver. Consistent with the pattern of *en* expression, ~50% of the stage 12 embryos showed a 14-stripe pattern (Figure 6A). This result confirmed the functionality of the *UAS-crc* construct and confirmed hybridization of the antisense probe to *crc* mRNAs. The remaining embryos showed lower, ubiquitous hybridization (Figure 6B), and this signal was detectable prior to the onset of zygotic transcription. Comparable ubiquitous staining was observed in wild-type embryos (data not shown). Thus, *crc* transcripts appear to be maternally loaded. No signal was detected with the sense *crc* probe (Figure 6C).

In wild-type, wandering stage third instar larvae, we observed specific hybridization in several tissues (Figure 7). The imaginal discs and CNS displayed the strongest signals. There was strong, relatively uniform staining in the T1-T3 leg discs and detectable, though weaker, staining in the wing discs, labial discs, and in large cells associated with the anterior spiracles. Within the CNS, the strongest expression was observed in or near the optic lobe proliferation zones (Figure 8A). The rest of the brain and ventral nerve cord showed strong, uni-

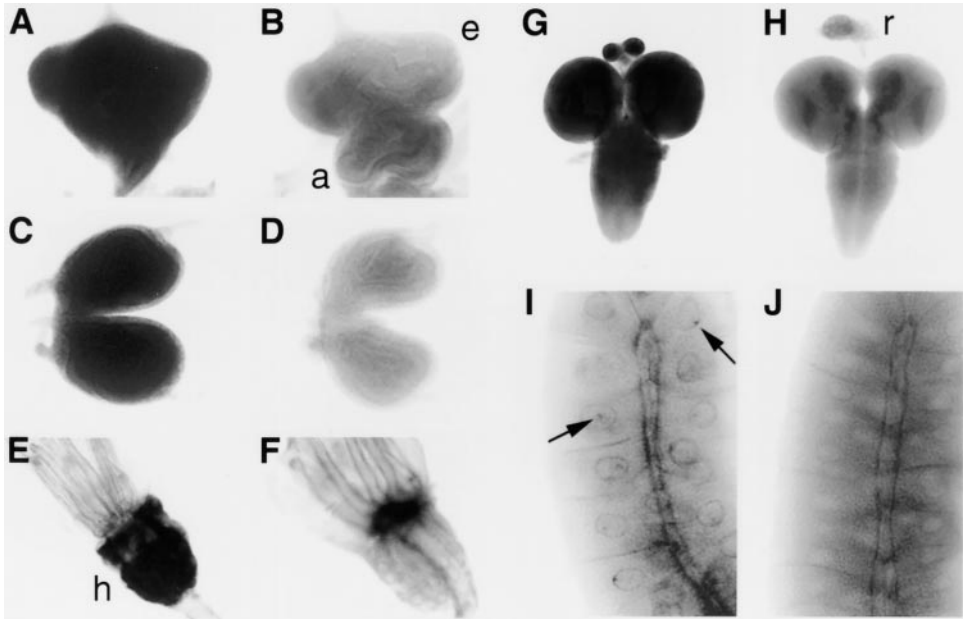

Figure 7.—Whole-mount *crc in situ* hybridization in wild-type third instar larvae. (A, C, E, G, and I) Antisense *crc* mRNA probe. (B, D, F, H, and J) Sense probe. (A and B) Eye (e) and antennal (a) discs. (C and D) T1 leg discs. (E and F) Cells associated with the anterior spiracles (h). (G and H) CNS and ring gland (r). (I and J) Salivary gland. Arrows, small patches of strong staining within the large salivary gland nuclei.

form hybridization, although less hybridization was observed in the posterior abdominal neuromeres. We also observed specific hybridization in patches of small cells located throughout the midgut (data not shown).

We examined the effects of several *crc* alleles on the pattern of *crc in situ* hybridization in the CNS of feeding third instar larvae (Figure 8). There was strong hybridization in the CNS of *+/Rev8* larvae (Figure 8A). By contrast, no signal was detected in larvae bearing a complete deletion of the *crc* locus (*Rev8/Rev4*, data not shown), nor was there signal in *R6/Rev8* (Figure 8B) and *R1/Rev8* (Figure 8C) larvae. Both *R1* and *R6* delete portions of *crc*-a, but *R1* and *R6* may have differential effects on *crc*-b/c (Figure 1A). Thus, under the hybridization and detection conditions used for this experiment, it appears that the *crc*-a isoform accounts for most if not all of the visible signal, while *crc*-b and *crc*-c were below detection. Finally, the pattern of hybridization in crc^1*/Rev8* larvae (Figure 8D) was the same as the pattern observed in the control, *+/Rev8* larvae (Figure 8A). Thus, *crc* expression in the CNS appeared to be normal in crc^1 mutants, consistent with our interpretation that a defect at the protein level ($Q^{171}R$) likely accounts for the crc^1 mutant phenotype.

DISCUSSION

The *crc* gene encodes multiple ATF4-like protein isoforms: *crc* is a complex locus encoding multiple mRNA and protein isoforms. The two most abundant forms are CRC-A and CRC-B; on the basis of their representation among ESTs, the transcripts encoding CRC-A outnumber those encoding CRC-B by approximately nine to one. Consistent with this observation, most of the *in situ* hybridization signal observed with a probe for both isoforms was attributable to the transcript encoding

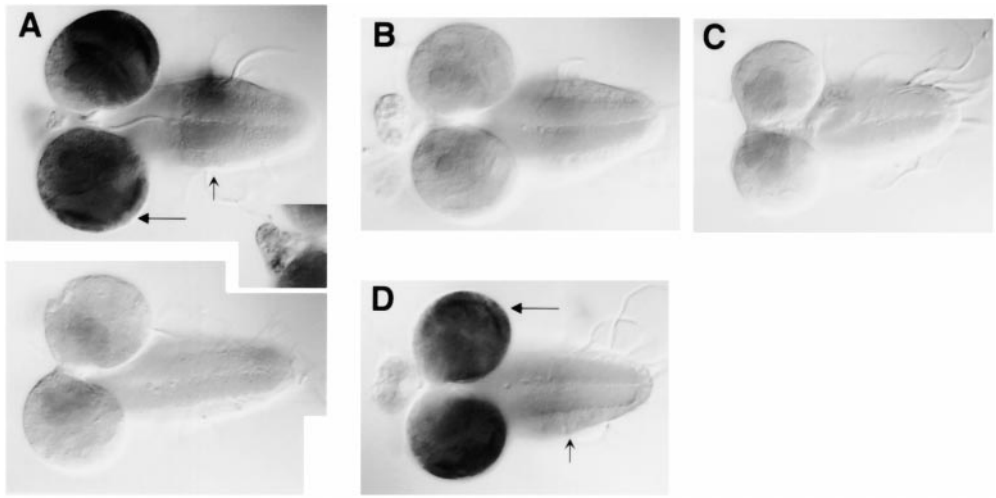

Figure 8.—*crc in situ* hybridization in crc^1 mutants. In this experiment, the color reaction was not allowed to proceed as far as in Figure 7. (A) *y w; Rev8/CyO, y^+* with antisense (top) and sense (bottom) *crc* RNA probes. (B) *y w; al dp R6/Rev8*. (C) *y w; R1/Rev8*. (D) *y w;* crc^1*/Rev8*. Inset in A, ring gland displaying weak but detectable hybridization; horizontal arrows, optic proliferation zones; vertical arrows, border of stronger, uniform hybridization in the anterior ventral nervous system.

CRC-A (Figure 8). CRC-A and CRC-B differ at the N terminus, while a common C-terminal region contains identical bZIP protein dimerization and DNA-binding domains. Therefore, CRC-A and CRC-B likely share dimerization partners and show identical DNA-binding properties.

In addition to the two major mRNA isoforms, there were three uncommon transcripts, *crc*-d–f, which may serve regulatory functions. *crc*-d encodes CRC-D, a C-terminally truncated form of CRC-A. Therefore, CRC-D lacks the bZIP domain and could function as a dominant negative regulator by competing with CRC-A (or other factors) for protein-binding sites. The expression of CRC-D may be essential for viability; the crc^{E85} mutation, which partially deletes a CRC-D-specific exon, displays significant lethality. The *crc*-e and *crc*-f transcripts have very small open reading frames that are preceded by suboptimal translational start sites, indicating that they may not be efficiently translated. Rather, these transcripts may participate in the regulation of the *crc* gene (*e.g.*, Smith *et al.* 1989). For mammalian CREB, the expression of truncated forms has been proposed to interrupt a positive feedback loop involving autoactivation of the gene (Waeber *et al.* 1991). Therefore, similar mechanisms may be involved in the regulation of *crc* expression.

Isoform-specific mutations reveal multiple *crc* gene functions: Genetic analysis demonstrated that *crc* is a complex locus consisting of at least two overlapping lethal complementation groups (Table 1). These complementation groups correlate with the molecular structure of the *crc* gene, indicating that the different CRC protein isoforms have overlapping, but distinct functions. We propose the following hypothesis to explain the correlation between the molecular and genetic results. The 3′ complementation group phenotypes reflect the functions of both CRC-A and CRC-B. Consistent with this prediction, the one observed sequence alteration in crc^{1} ($Q^{171}R$) was found in a region common to CRC-A and CRC-B. The 5′ group phenotypes reflect CRC-A- and/or CRC-D-specific functions that do not require CRC-B.

Nevertheless, we anticipate some overlap in the functions of the different CRC proteins. The lethal phenotypes of both *crc* complementation groups were rescued by ectopic expression of a single RNA isoform encoding CRC-B. Furthermore, the C-terminal 288 amino acids of CRC-A and CRC-B are identical, and both lethal complementation groups displayed similar defects in leg disc elongation. *R6*, which deleted this common region, failed to complement both 5′ and 3′ group alleles.

***crc* performs critical functions during molting and metamorphosis:** *crc* mutant alleles displayed several defects associated with molting and metamorphosis. The mutant phenotypes associated with the two lethal complementation groups were distinct, although there was some overlap. Therefore, these mutations define multiple roles for *crc* during development.

In insects, the molts between successive larval stages are initiated and coordinated by pulses of ecdysone (Riddiford 1993). This process appears to require *crc*. As previously described for the crc^{1} allele (Chadfield and Sparrow 1985), both crc^{1} and *R6* displayed larval lethality associated with failure to shed the old larval mouthparts (Figure 4G). These alleles comprise the 3′ complementation group and involve disruptions common to the *crc*-a, *crc*-b, and *crc*-c transcripts. Therefore, CRC-A and/or CRC-B perform an important role(s) in the regulation of larval molting. Similar larval phenotypes have been described for mutations in the *dare* gene, which encodes an adrenodoxin reductase likely to be involved in ecdysone biosynthesis (Freeman *et al.* 1999). Likewise, mutants in *EcR-B*, which is a component of heterodimeric ecdysone receptors, and PHM, an enzyme involved in neuropeptide biosynthesis, both displayed this larval molting phenotype (Schubiger *et al.* 1998; Jiang *et al.* 2000). These similarities indicate that CRC-A and CRC-B may perform necessary functions in the peptidergic neurons that stimulate ecdysone biosynthesis, in the ecdysone-producing prothoracic gland cells, and/or in the tissues that respond to the ecdysone signal.

During the third larval instar, pulses of ecdysone trigger the onset of metamorphosis (Thummel 1996). A late high titer pulse of ecdysone triggers puparium formation. Approximately 12 hr later, a subsequent brief pulse of ecdysone directs pupation. *crc* mutants displayed defects in pupariation and pupation, indicating that both of these developmental transitions require *crc*. The pupariation defects seen in *R6* hemizygotes (Figure 4H)—retention of the larval shape, failure to form the abdominal gas bubble, and incomplete eversion of the anterior spiracles—are reminiscent of similar defects described for late-arrested *EcR-B* mutants (Schubiger *et al.* 1998) and for mutations in *E74B* (Fletcher *et al.* 1995) and *DHR3* (Lam *et al.* 1999).

At pupation, crc^{1} and *R6* both displayed the cryptocephal phenotype as well as defects in imaginal disc elongation (*e.g.*, Figure 4, A–D). Similar pupation defects are associated with mutations in several ecdysone-response genes, including *E74B* (Fletcher *et al.* 1995), *crol* (D'Avino and Thummel 1998), β*FTZ-F1* (Broadus *et al.* 1999), *DHR3* (Lam *et al.* 1999), and the *BR-C* (Kiss *et al.* 1988). Unlike crc^{1} and *R6*, the leg and wing discs in the 5′ group mutants remained bulbous and undifferentiated, and often discolored. A phenotype similar to that of 5′ group mutants has been reported for β*FTZ-F1* (Broadus *et al.* 1999). Therefore, lesions in *crc* and the ecdysone-response genes generate common defects in the larval, prepupal, and pupal responses to ecdysone signaling. These similarities indicate that *crc* has a central role in the regulation of ecdysone biosynthesis/secretion or in determining the responses of target tis-

sues to the steroid signals. As an important next step in our analysis of *crc* function, we plan to examine whether *crc* is also an ecdysone-response gene.

After comparing aspects of the *E74B* pupal phenotype and the phenotypes of mutations affecting larval muscle development, Fletcher *et al.* (1995) proposed that premature death of the larval muscles might account for the defects observed at pupariation and pupation in those mutants. Due to similarities in phenotype between *E74B* and *crc*, this model could also account for the pupariation and pupation defects observed in *crc* mutants, but it probably does not explain the *crc* larval molting and adult fecundity defects. Moreover, as is true for *E74B* (Fletcher *et al.* 1995), most crc^1 and *R6* mutants display normal larval locomotion (R. S. Hewes, unpublished observations), indicating that the larval muscles develop and function normally prior to metamorphosis.

Rescue of *crc* by germ-line transformation: Transgenic *UAS-crc* lines rescued the lethal phenotype of both the 5′ and 3′ lethal complementation groups (*929* and crc^1), confirming the identification of *crc*. The rescue was partial, and some aspects of the mutant phenotype, such as the reduction in female fecundity and the defects in adult wing expansion and tanning, showed no improvement. Several factors may have contributed to the incomplete rescue. These include requirements for expression of the CRC-A and CRC-D isoforms, or for more precise temporal and/or spatial regulation of CRC expression.

One aspect of the rescue experiments did not fit simple predictions but may be explained by technical details of the transgene expression. The rank order of potency for the rescue of crc^1 by the different *UAS-crc* lines was reversed for the rescue of *929*. The variation in the degree of crc^1 rescue was likely due to position effects that led to constitutive, low level expression of the transgene. By contrast, *c929* is an enhancer trap *P* element that drives heterogeneous GAL4 reporter gene expression in several tissues. Thus, to explain the second observation, *c929* may rescue the wild-type pattern of *crc* expression to a significant degree, while minimizing the negative effects of *crc* misexpression in other tissues.

Potential interactions between *crc* and ecdysone signaling pathways: By analogy to other CREB/ATF proteins, the roles of *crc* during molting and metamorphosis are likely to involve heterodimerization with other bZIP proteins and competition with them for DNA-binding sites (Hai and Curran 1991). Similarly, we hypothesize that ecdysone-responsive signaling pathways include *crc*. For example, by convergence on the transcriptional coactivator, CREB-binding protein (CBP), CREB/ATF proteins can antagonize the activity of members of the nuclear receptor superfamily (Kamei *et al.* 1996). This family includes several ecdysone-response genes. Therefore, further analysis of *crc* may elucidate several points of interaction between *crc* and these hormonal signaling pathways.

We thank Rod Murphey, David Shepherd, Carl Thummel, Ian Duncan, Haig Keshishian, and the Berkeley Drosophila Genome Project for fly stocks. We also thank the Berkeley Drosophila Genome Project/HHMI EST Project for ESTs and genomic sequences. We are grateful to Mike Horner, Carl Thummel, Martin Burg, and William Pak for the sharing of information, clones, and fly stocks from 39C4, John Tamkun for the genomic libraries, and Paul Salvaterra, Gerald Rubin, and Bruce Hamilton for cDNA libraries. We thank Sonalee Jilhewar, Marie Roberts, and Dimitri Reznikov for technical assistance and Dianne Duncan for advice with *in situ* hybridization. This work was supported by National Institutes of Health grant NS21749 (P.H.T.) and American Cancer Society Postdoctoral Fellowship PF4212 (R.S.H.).

LITERATURE CITED

Andres, A. J., and C. S. Thummel, 1995 The Drosophila 63F early puff contains *E63-1*, an ecdysone-inducible gene that encodes a novel Ca(2+)-binding protein. Development **121:** 2667–2679.

Bainbridge, S. P., and M. Bownes, 1981 Staging the metamorphosis of *Drosophila melanogaster*. J. Embryol. Exp. Morphol. **66:** 57–80.

Bartsch, D., M. Ghirardi, P. A. Skehel, K. A. Karl, S. P. Herder *et al.*, 1995 Aplysia CREB2 represses long-term facilitation: relief of repression converts transient facilitation into long-term functional and structural change. Cell **83:** 979–992.

Beneviste, R. J., and P. H. Taghert, 1999 Cell type-specific regulatory sequences control expression of the Drosophila *FMRF-NH$_2$* neuropeptide gene. J. Neurobiol. **38:** 507–520.

Brand, A. H., and N. Perrimon, 1993 Targeted gene expression as a means of altering cell fates and generating dominant phenotypes. Development **118:** 401–415.

Broadus, J., J. R. McCabe, B. Endrizzi, C. S. Thummel and C. T. Woodard, 1999 The Drosophila βFTZ-F1 orphan nuclear receptor provides competence for stage-specific responses to the steroid hormone ecdysone. Mol. Cell **3:** 143–149.

Burtis, K. C., C. S. Thummel, C. W. Jones, F. D. Karim and D. S. Hogness, 1990 The Drosophila 74EF early puff contains *E74*, a complex ecdysone-inducible gene that encodes two ets-related proteins. Cell **61:** 85–99.

Cavener, D. R., and S. C. Ray, 1991 Eukaryotic start and stop translation sites. Nucleic Acids Res. **19:** 3185–3192.

Chadfield, C. G., and J. C. Sparrow, 1985 Pupation in *Drosophila melanogaster* and the effect of the *lethalcryptocephal* mutation. Dev. Genet. **5:** 103–114.

Crossgrove, K., C. A. Bayer, J. W. Fristrom and G. M. Guild, 1996 The Drosophila *Broad-Complex* early gene directly regulates late gene transcription during the ecdysone-induced puffing cascade. Dev. Biol. **180:** 745–758.

D'Avino, P. P., and C. S. Thummel, 1998 *crooked legs* encodes a family of zinc finger proteins required for leg morphogenesis and ecdysone-regulated gene expression during Drosophila metamorphosis. Development **125:** 1733–1745.

DiBello, P. R., D. A. Withers, C. A. Bayer, J. W. Fristrom and G. M. Guild, 1991 The Drosophila Broad-Complex encodes a family of related proteins containing zinc fingers. Genetics **129:** 385–397.

Estes, S. D., D. L. Stoler and G. R. Anderson, 1995 Normal fibroblasts induce the C/EBP beta and ATF-4 bZIP transcription factors in response to anoxia. Exp. Cell Res. **220:** 47–54.

Fawcett, T. W., J. L. Martindale, K. Z. Guyton, T. Hai and N. J. Holbrook, 1999 Complexes containing activating transcription factor (ATF)/cAMP-responsive-element-binding protein (CREB) interact with the CCAAT/enhancer-binding protein (C/EBP)-ATF composite site to regulate Gadd153 expression during the stress response. Biochem. J. **339:** 135–141.

Felsenstein, J., 1993 PHYLIP (Phylogeny Inference Package) version 3.5c. Distributed by the author. Department of Genetics, University of Washington, Seattle.

Fletcher, J. C., K. C. Burtis, D. S. Hogness and C. S. Thummel,

1995 The Drosophila *E74* gene is required for metamorphosis and plays a role in the polytene chromosome puffing response to ecdysone. *Development* **121:** 1455–1465.

Freeman, M. R., A. Dobritsa, P. Gaines, W. A. Segraves and J. R. Carlson, 1999 The *dare* gene: steroid hormone production, olfactory behavior, and neural degeneration in Drosophila. Development **126:** 4591–4602.

Fristrom, J. W., 1965 Development of the morphological mutant *cryptocephal* of *Drosophila melanogaster*. Genetics **52:** 297–318.

Gelbart, W. M., M. Crosby, B. Matthews, W. P. Rindone, J. Chillemi *et al.*, 1997 FlyBase: a Drosophila database. The FlyBase consortium. Nucleic Acids Res. **25:** 63–66.

Gloor, G. B., C. R. Preston, D. M. Johnson-Schlitz, N. A. Nassif, R. W. Phillis *et al.*, 1993 Type I repressors of *P* element mobility. Genetics **135:** 81–95.

Hadorn, E., and H. Gloor, 1943 Cryptocephale in spat wirkender Letalfaktor bei *Drosophila melanogaster*. Revue suisse Zool. **50:** 256–261.

Hai, T., and T. Curran, 1991 Cross-family dimerization of transcription factors Fos/Jun and ATF/CREB alters DNA binding specificity. Proc. Natl. Acad. Sci. USA **88:** 3720–3724.

Halfon, M. S., H. Kose, A. Chiba and H. Keshishian, 1997 Targeted gene expression without a tissue-specific promoter: creating mosaic embryos using laser-induced single-cell heat shock. Proc. Natl. Acad. Sci. USA **94:** 6255–6260.

Jiang, C., E. H. Baehrecke and C. S. Thummel, 1997 Steroid regulated programmed cell death during Drosophila metamorphosis. Development **124:** 4673–4683.

Jiang, N., A. S. Kolhekar, P. S. Jacobs, R. E. Mains, B. A. Eipper *et al.*, 2000 *PHM* is required for normal developmental transitions and for biosynthesis of secretory peptides in Drosophila. Dev. Biol. (in press).

Kamei, Y., L. Xu, T. Heinzel, J. Torchia, R. Kurokawa *et al.*, 1996 A CBP integrator complex mediates transcriptional activation and AP-1 inhibition by nuclear receptors. Cell **85:** 403–414.

Kawai, T., M. Matsumoto, K. Takeda, H. Sanjo and S. Akira, 1998 ZIP kinase, a novel serine/threonine kinase which mediates apoptosis. Mol. Cell. Biol. **18:** 1642–1651.

Kiss, I., A. H. Beaton, J. Tardiff, D. Fristrom and J. W. Fristrom, 1988 Interactions and developmental effects of mutations in the Broad-Complex of *Drosophila melanogaster*. Genetics **118:** 247–259.

Lam, G., B. L. Hall, M. Bender and C. S. Thummel, 1999 *DHR3* is required for the prepupal-pupal transition and differentiation of adult structures during Drosophila metamorphosis. Dev. Biol. **212:** 204–216.

Lindsley, D. L., and G. G. Zimm, 1992 *The Genome of Drosophila melanogaster*. Academic Press, New York.

Mielnicki, L. M., R. G. Hughes, P. M. Chevray and S. C. Pruitt, 1996 Mutated Atf4 suppresses c-Ha-ras oncogene transcript levels and cellular transformation in NIH3T3 fibroblasts. *Biochem. Biophys. Res. Commun.* **228:** 586–595.

O'Brien, M. A., and P. H. Taghert, 1998 A peritracheal neuropeptide system in insects: release of myomodulin-like peptides at ecdysis. J. Exp. Biol. **201:** 193–209.

O'Brien, M. A., M. S. Roberts and P. H. Taghert, 1994 A genetic and molecular analysis of the 46C chromosomal region surrounding the *FMRFamide* neuropeptide gene in *Drosophila melanogaster*. Genetics **137:** 121–137.

Pirrotta, V., 1986 Cloning Drosophila genes, pp. 83–110 in *Drosophila: A Practical Approach*, edited by D. B. Roberts. IRL Press, Oxford, England.

Preston, C. R., J. A. Sved and W. R. Engels, 1996 Flanking duplications and deletions associated with *P*-induced male recombination in Drosophila. Genetics **144:** 1623–1638.

Restifo, L. L., and K. White, 1991 Mutations in a steroid hormone-regulated gene disrupt the metamorphosis of the central nervous system in Drosophila. Dev. Biol. **148:** 174–194.

Riddiford, L. M., 1993 Hormones and Drosophila development, pp. 899–939, in *The Development of Drosophila melanogaster*, Vol. II, edited by M. Bate and A. Martinez Arias. Cold Spring Harbor Laboratory Press, Cold Spring Harbor, NY.

Rodgers, S., R. Wells and M. Rechsteiner, 1986 Amino acid sequences common to rapidly degraded proteins: the PEST hypothesis. Science **234:** 364–368.

Sambrook, J., E. F. Fritsch and T. Maniatis, 1989 *Molecular Cloning: A Laboratory Manual*. Cold Spring Harbor Laboratory Press, Cold Spring Harbor, NY.

Schaefer, A. M., and P. H. Taghert, 1995 A Drosophila gene required for the viability or normal function of diverse neuropeptide neurons. Soc. Neurosci. Abst. **21:** 255.8.

Schubiger, M., A. A. Wade, G. E. Carney, J. W. Truman and M. Bender, 1998 Drosophila EcR-B ecdysone receptor isoforms are required for larval molting and for neuron remodeling during metamorphosis. Development **125:** 2053–2062.

Segraves, W. A., and D. S. Hogness, 1990 The *E75* ecdysone-inducible gene responsible for the 75B early puff in Drosophila encodes two new members of the steroid receptor superfamily. Genes Dev. **4:** 204–219.

Smith, C. W., J. G. Patton and B. Nadal-Ginard, 1989 Alternative splicing in the control of gene expression. Annu. Rev. Genet. **23:** 527–577.

Sparrow, J. C., and C. G. Chadfield, 1982 Chitin biosynthesis during pupal development of *Drosophila melanogaster* and the effect of the *lethalcryptocephal* mutation. Dev. Genet. **3:** 235–245.

Spradling, A. C., D. M. Stern, I. Kiss, J. Roote, T. Laverty *et al.*, 1995 Gene disruptions using P transposable elements: an integral component of the Drosophila genome project. Proc. Natl. Acad. Sci. USA **92:** 10824–10830.

Spradling, A. C., D. Stern, A. Beaton, E. J. Rhem, T. Laverty *et al.*, 1999 The Berkeley Drosophila Genome Project gene disruption project: single *P*-element insertions mutating 25% of vital Drosophila genes. Genetics **153:** 135–177.

Sved, J. A., W. B. Eggleston and W. R. Engels, 1990 Germ-line and somatic recombination induced by in vitro modified *P* elements in *Drosophila melanogaster*. Genetics **124:** 331–337.

Tautz, D., and C. Pfeifle, 1989 A non-radioactive in situ hybridization method for the localization of specific RNAs in Drosophila embryos reveals translational control of the segmentation gene *hunchback*. Chromosoma **98:** 81–85.

Thummel, C. S., 1996 Flies on steroids – Drosophila metamorphosis and the mechanisms of steroid hormone action. Trends Genet. **12:** 306–310.

Truman, J. W., W. S. Talbot, S. E. Fahrbach and D. S. Hogness, 1994 Ecdysone receptor expression in the CNS correlates with stage-specific responses to ecdysteroids during Drosophila and Manduca development. Development **120:** 219–234.

Urness, L. D., and C. S. Thummel, 1995 Molecular analysis of a steroid-induced regulatory hierarchy: the Drosophila E74A protein directly regulates *L71-6* transcription. EMBO J. **14:** 6239–6246.

Vinson, C. R., T. Hai and S. M. Boyd, 1993 Dimerization specificity of the leucine zipper-containing bZIP motif on DNA binding: prediction and rational design. Genes Dev. **7:** 1047–1058.

Waeber, G., T. E. Meyer, M. LeSieur, H. L. Hermann, N. Gerard *et al.*, 1991 Developmental stage-specific expression of cyclic adenosine 3′, 5′-monophosphate response element-binding protein CREB during spermatogenesis involves alternative exon splicing. Mol. Endocrinol. **5:** 1418–1430.

Wright, T. R. F., R. B. Hodgetts and A. F. Sherald, 1976 The genetics of dopa decarboxylase in *Drosophila melanogaster*. Genetics **84:** 267–285.

Communicating editor: R. S. Hawley